Closing of the Mott gap near step edges in NiS_2

Yuuki Yasui,[1,2,*] Kota Iwata,[2] Shota Okazaki,[3] Shigeki Miyasaka,[4] Yoshiaki Sugimoto,[2] Tetsuo Hanaguri,[1,†] Hidenori Takagi,[5,6,7] and Takao Sasagawa[3,8]

[1]*RIKEN Center for Emergent Matter Science, Wako, Saitama 351-0198, Japan*
[2]*Department of Advanced Materials Science, The University of Tokyo, Kashiwa, Chiba 277-8561, Japan*
[3]*Laboratory for Materials and Structures, Tokyo Institute of Technology, Yokohama, Kanagawa 226-8501, Japan*
[4]*Department of Physics, Osaka University, Toyonaka, Osaka 560-0043, Japan*
[5]*Department of Physics, Graduate School of Science, The University of Tokyo, Bunkyo, Tokyo 113-0033, Japan*
[6]*Institute for Functional Matter and Quantum Technologies, University of Stuttgart, 70569 Stuttgart, Germany*
[7]*Max Planck Institute for Solid State Research, Heisenbergstraße 1, 70569 Stuttgart, Germany*
[8]*Research Center for Autonomous Systems Materialogy, Tokyo Institute of Technology, Yokohama, Kanagawa 226-8501, Japan*

(Received 11 April 2024; accepted 21 June 2024; published 19 July 2024)

A prototypical charge-transfer type Mott insulator NiS_2 pyrite exhibits a metal-insulator transition with bandwidth control. Recent discoveries on surface-specific electronic states on other 3*d* transition-metal disulfide pyrites motivate us to further investigate the surface of NiS_2, where metallic surface conduction is discussed. Here, the spectroscopic-imaging scanning-tunneling-microscopy observations revealed that the surface is not metallic, contrary to the expectation. Instead, the Mott gap is closed near step edges, suggesting possible electrical conduction from one-dimensional channels. The edge anomaly was observed irrespective of its magnetic order and is limited to the insulator phases.

DOI: 10.1103/PhysRevB.110.045139

I. INTRODUCTION

Transition-metal (TM) disulfides in the pyrite structure, in which TM^{2+} and S_2^{2-} crystalize in the NaCl structure with space group $Pa\bar{3}$ [Figs. 1(a) and 1(b)], offer a variety of electric and magnetic properties depending on its *d*-band filling [1–3]. FeS_2 ($t_{2g}^6 e_g^0$) is a diamagnetic semiconductor, CoS_2 ($t_{2g}^6 e_g^1$) is a ferromagnetic metal, NiS_2 ($t_{2g}^6 e_g^2$) is an antiferromagnetic Mott insulator with half-filled e_g bands, CuS_2 ($t_{2g}^6 e_g^3$) is a superconductor, and ZnS_2 ($t_{2g}^6 e_g^4$) is a semiconductor.

NiS_2 undergoes a metal-to-insulator transition with bandwidth control, and it is considered to be a typical model as it does not change the crystal structure [4]. The bandwidth control is achieved by Se substitution with S [5–9] and an application of hydrostatic pressure [10,11]. The pristine NiS_2 at an ambient pressure exhibits a noncolinear antiferromagnetic order below 39 K, and a weak ferromagnetic order below 30 K [Fig. 1(c)].

The resistivity of NiS_2 tends to saturate at low temperatures even though it is an insulator. It has been argued that the surface may be metallic and dominate the electric conduction at low temperatures [14]. The multichannel conductance is supported by changing the crystalline grain size [15] and with heat treatments [16]. The neutron scattering measurements with susceptibility measurements suggest the surface contributes also to its magnetic state [17]. Additionally, a finite density of states (DOS) at the Fermi level by the photoemission spectroscopy [7,18] further implies its metallic surface states. More recent research has focused on the surface anomalies convince the additional metallic channel [19] and imply magnetic anomalies at step edges [20,21].

As surface conduction is implied in NiS_2, it is interesting to investigate the surface directly by using the spectroscopic-imaging scanning tunneling microscopy (STM). An STM observation was reported for the metallic compounds $NiS_{2-x}Se_x$ ($x \geqslant 0.45$) [22] whereas its insulating state has not been investigated. In this article, we report STM results for the Mott insulating side ($x = 0$ and 0.45). In the three-dimensional (3D) crystal structure, we find that its two-dimensional (2D) surface is indeed insulating, contrary to the expectation from previous reports. Interestingly, the Mott gap becomes smaller as approaches to one-dimensional (1D) step edges in the weak ferromagnetic insulator (WFI) and the paramagnetic insulator (PI) phases. Thus, we infer that the suggested conductance is happening at the 1D step edges rather than 2D surfaces. Such edge effect was not observed in Se substituted metallic crystals $NiS_{1.55}Se_{0.45}$.

II. METHODS

$NiS_{2-x}Se_x$ ($x = 0$ and 0.45) single crystals were grown with the chemical vapor transport method [6]. For STM measurements at 77 K, the samples were cleaved in an ultrahigh vacuum chamber ($\sim 10^{-8}$ Pa) at around 77 K to expose clean and flat (0 0 1) surfaces and then transferred to a microscope without breaking vacuum. As scanning tips, tungsten wires were used after electrochemical etching in KOH aqueous solution, followed by tuning using field ion microscopy and controlled indentation at clean Cu(1 1 1) surfaces. Measurements at 5 K were performed with

*Contact author: yasui@k.u-tokyo.ac.jp
†Contact author: hanaguri@riken.jp

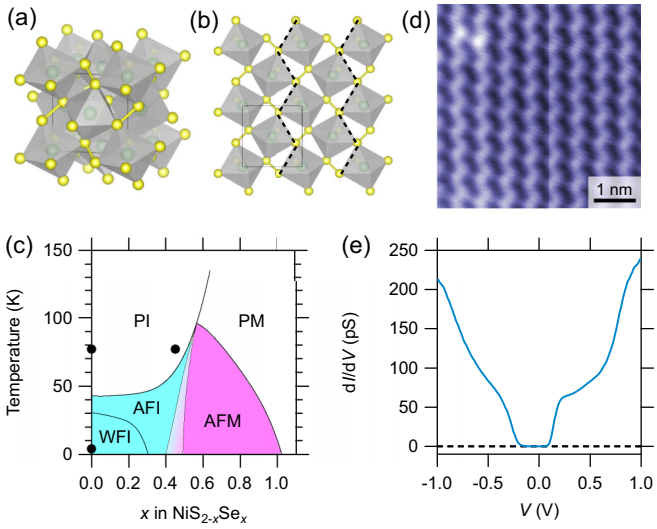

FIG. 1. (a) The crystal structure of NiS_2 [12,13]. Ni atoms are represented in green, and S atoms are in yellow. (b) A model for a cleaved surface seen from the *c*-axis. The zigzag structure of the topmost S atoms is highlighted with dashed lines. (c) A schematic phase diagram of $NiS_{2-x}Se_x$ reproduced from [5]. PM, paramagnetic metal; AFI, antiferromagnetic insulator. The conditions investigated in the present study are marked by black dots. (d) A constant-current topographic image of NiS_2. (e) A spatially averaged dI/dV spectrum at a 2D surface. The set-point bias voltage $V_s = +1$ V, set-point current $I_s = 100$ pA, and measurement temperature $T = 77$ K.

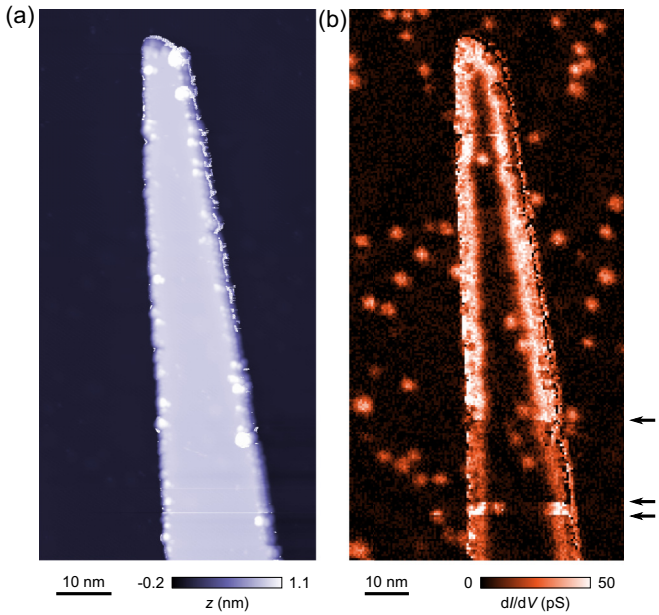

FIG. 2. Edge states in NiS_2 measured at 77 K (PI phase). (a) A topographic image of a pseudoisland structure. (b) A dI/dV map at +200 mV within the surface Mott gap taken in the same field of view as (a). Positions where the tip changed are marked with black arrows. $V_s = +0.9$ V and $I_s = 100$ pA.

the Omicron low-temperature scanning tunneling microscopy (LT-STM) system. The crystals were cleaved in the ultra-high vacuum chamber at room temperature. A tungsten tip attached to a qPlus sensor was used after controlled indentation at clean Au(1 1 1) surfaces. Tunneling-conductance dI/dV curves were obtained with numerical differentials of tunneling current I versus bias voltage V curves.

III. RESULTS

An STM topographic image of the cleaved surface is shown in Fig. 1(d). One type of surface is available in this material because the S-S dimer bonds may not be broken. The zigzag structure does not contradict the model structure as in Fig. 1(b). The observed lattice constant is around 560 pm, which agrees with the literature value of NiS_2 [23].

Tunneling conductance curves were measured on such cleaved surfaces at 77 K, in the PI phase [Fig. 1(e)]. The observed dI/dV spectra are approximately proportional to the local DOS, and hence we can directory refer to the insulating gap. The measured insulating gap width is about 0.3 eV at 77 K, which is comparable to the reported gap width of the bulk [24]. Contrary to the speculations of the previous reports [7,14–19], the 2D surfaces are found to be insulating.

As the surface of NiS_2 is found to be insulating, metallic states may originate from some defects or from some specific structures. We investigated the electronic states near step edges because the lack of a good cleavage plane in NiS_2 results in a large number of step-terrace structures at cleavages. The electronic state just below step edges cannot be investigated with STM since a finite radius of a scanning tip causes tunneling current through the side of the tip. Such artifacts of the tip shape are avoided on terraces above steps. Thus, we focus on the electronic states above the steps in the following, and the data are considered only for the topographic height $|z| < 50$ pm.

A step-terrace structure with two-unit-cell hight [Fig. 2(a)] was investigated with the spectroscopic-imaging technique, where the dI/dV conductance curves are measured at each pixel of the image. Figure 2(b) shows a dI/dV map at +200 mV, representing the local DOS distribution within the insulating gap. The in-gap states appear all around the step edges. Thus, the behavior is not constrained to a specific orientation of the step with respect to the crystalline axis. Although the tip condition changed several times during the measurements as marked with black arrows, the in-gap state is observed irrespective of the tip condition.

A magnified view shows a more detailed structure of the in-gap states. The step was obtained from the same crystal at a different cleavage, and the step height corresponds to 1 unit cell. The topographic image is shown in Fig. 3(a), and a DOS map at +200 mV representing the in-gap edge states is shown in Fig. 3(b). These images are deformed due to the thermal drift but the atomic registry is maintained. Figure 3(c) compares the tunneling spectra near and away from the step edge. The insulating gap is almost closed near the step edge, resulting in a quasimetallic state in the 1D step edge. The spatial distribution of the tunneling spectra near the step edge is shown in Figs. 3(d) to 3(f). The in-gap states near the step edge are not restricted to the step edge, but they spread over several nanometers into the terrace.

Some bright spots in dI/dV are observed on the terraces [Fig. 2(b)]. These spots probably originated from impurities

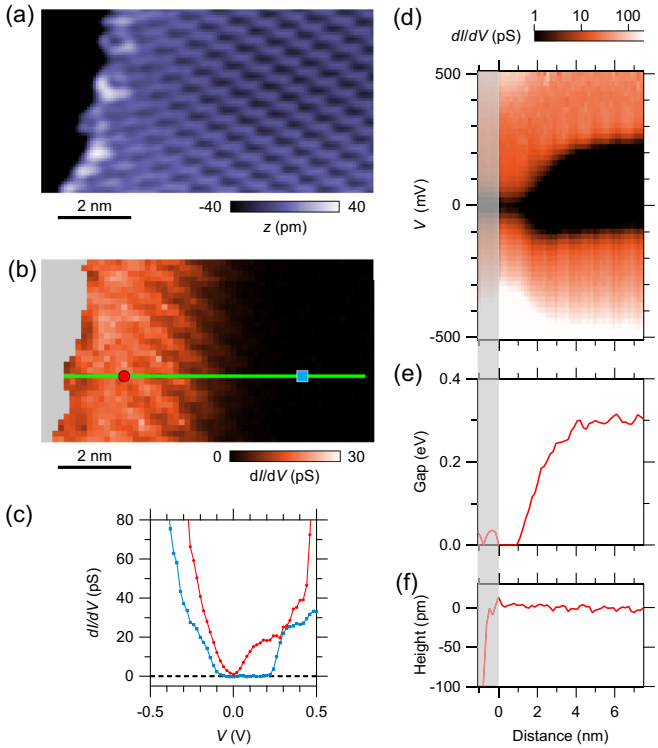

FIG. 3. The edge anomaly in NiS_2 measured at 77 K (PI phase). (a) A topographic image near a step edge. (b) A dI/dV map at +200 mV within the surface Mott gap taken in the same field of view as (a). Points at $z < -50$ pm are not shown. (c) dI/dV spectra near (red circle) and away (blue square) from the step edge. (d) Tunneling conductance spectra along the green line in (b). (e) The variation of the insulating gap defined at 1 pS. (f) The line profile of the simultaneously taken topographic image. $V_s = +1.0$ V and $I_s = 100$ pA.

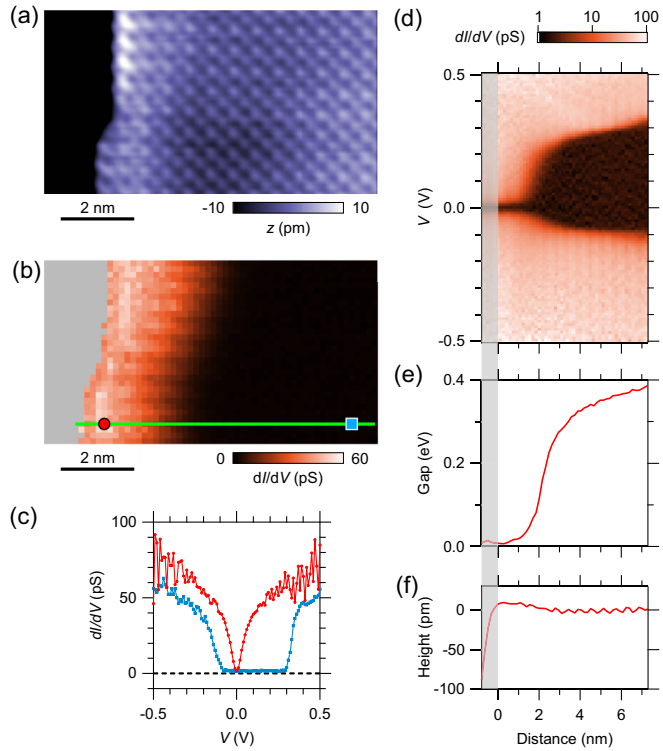

FIG. 4. The edge anomaly in NiS_2 measured at 5 K (WFI phase). (a) A topographic image near a step edge. The image is Fourier-filtered to suppress high-frequency noise. (b) A dI/dV map at +200 mV within the surface Mott gap in the same field of view as (a). Points at $z < -50$ pm are not shown. (c) dI/dV spectra near (red circle) and away (blue square) from the step. (d) Tunneling conductance spectra along the green line in (b). (e) The variation of the insulating gap defined at 2.5 pS. (f) The line profile of the simultaneously taken topographic image. $V_s = +1.5$ V and $I_s = 200$ pA.

embedded under the surface. Although the dI/dV spectra on these impurities are very similar to those near the step edges, it is unlikely that the observed gap collapse is associated with the impurities. This is because the in-gap states homogeneously distribute around step edges regardless of the position of impurities. Therefore, the metallic state is intrinsic to step edges of NiS_2.

The location of the gap with respect to the chemical potential depends on samples [compare Figs. 1(e) and 3(c)]. They probably originated from some doping effects from impurities. We confirmed that the gap closes toward the Fermi energy near step edges wherever the surface gap is.

To investigate the effect of magnetic order on the in-gap state near the step edge, we performed spectroscopic-imaging measurements near step edges also in the WFI phase at 5 K. A NiS_2 crystal from a different batch was used. Atomically sharp step edges are resolved in the topographic image in Fig. 4(a), where the tip probably feels the symmetry of Ni atoms as well. The step height is 4 nm, and the zigzag structure of S atoms is perpendicular to the step. As shown in Figs. 4(b) to 4(f), the insulating gap gradually collapses over a few nanometers as approaching the step edge, similar to the paramagnetic phase.

A natural question is whether the edge-induced effect is observed when the insulating gap is suppressed by the bandwidth control. To this end, we investigated $NiS_{2-x}Se_x$ (nominal $x = 0.45$), which is located around the boundary of the PI and the antiferromagnetic metal (AFM) phases [Fig. 1(c)]. As shown in Fig. 5, the topographic image exhibits two atomic sites with different heights. Se atoms are considered to appear higher in constant-current topographic images [22]. From the ratio between the numbers of higher and lower atoms on the surface, x is estimated to be 0.43, which agrees with the nominal amount of Se. A dI/dV map is measured at a step edge with 0.5-unit-cell hight [Figs. 5(a) and 5(b)]. There is no gap in the tunneling spectra as shown in Fig. 5(c). A line profile clarifies that any edge effect was not evident at any bias voltage within ±0.5 V [Figs. 5(d) to 5(f)].

IV. DISCUSSION

The surface conduction in NiS_2 has been proposed in the previous reports [14–17,19]. The present observations clarify that the 2D surfaces are as insulating as their bulk, and in fact, their 1D edges are more metallic. Since the in-gap states near step edges can provide an additional channel to the conductance, whose amount is directly related to the surface area, we consider that the previous observations are consistent for 1D edge conductance. The 1D edge channel can also infer

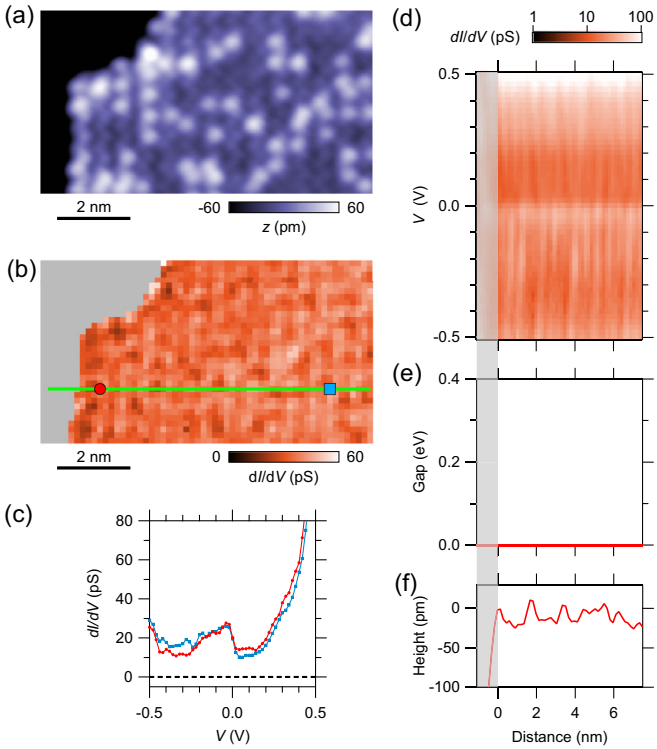

FIG. 5. Absence of a noticeable edge effect at the boundary of the PI and the AFM phases in $NiS_{1.55}Se_{0.45}$ measured at 77 K. (a) A topographic image near a step edge. Se atoms appear as bright protrusions while S atoms appear darker in the same zigzag structure. (b) A dI/dV map at +200 mV in the same field of view as (a). Points at $z < -50$ pm are not shown. (c) dI/dV spectra near (red circle) and away (blue square) from the step. (d) Tunneling conductance spectra along the green line in (b). (e) The variation of the insulating gap defined at 2.5 pS. (f) The line profile of the simultaneously taken topographic image. $V_s = +1.0$ V and $I_s = 100$ pA.

why the previous angle-resolved photoemission spectroscopy measurements did not report dispersive features within the Mott gap even though a finite DOS at the Fermi level is observed [7,9,18,25].

The question is what causes the observed metallic edge state. One possible scenario concerns a bandwidth-controlled Mott insulator-to-metal transition, which occurs when the onsite Coulomb repulsion U becomes smaller with respect to the bandwidth W. In bulk NiS_2, physical or chemical pressures induce the bandwidth-controlled Mott insulator-to-metal transition. However, U and W are expected to become larger and smaller, respectively, at the step edges due to weaker screening and hopping, which contradict the observed metallic edge state. Particular edge termination may effectively cause local doping, resulting in a metallic edge, as in the case of the metallic surface of $V_{2-x}Cr_xO_3$ with excess vanadyl cations [26]. In the present case, however, the metallic edge states appear irrespective of the edge direction, ruling out the possibility of a termination-dependent metallic state. Another possible cause of the metallic state is topological edge states [27–31]. Although the topological aspect of the band structure has theoretically been argued in NiS_2 for $U = 0$ [29], we are not aware of such an expectation for a more realistic situation with $U \neq 0$. More experimental and theoretical work is indispensable to clarify the underlying mechanism of the 1D metallic edge states in pyrite NiS_2.

V. CONCLUSIONS

In summary, the spectroscopic-imaging STM measurements on the charge-transfer-type Mott insulator NiS_2 clarified that the 2D surface is as gapped as the 3D bulk. The Mott gap collapses near the step edges in the WFI and the PI phases, exhibiting a quasimetallic DOS. This behavior was not observed at the phase boundary between the PI and the AFM phases. The spatially resolved results obtained in this work indicate that the surface conduction so far inferred from macroscopic measurements [14–16,19] are not related to the surface but associated with the step edges. Different types of "surface" effects have been found in various 3*d* transition-metal disulfides [32–38]. We anticipate that their systematic spatially-resolved investigations may help to understand the role of step edges in the pyrite structure.

ACKNOWLEDGMENTS

The authors acknowledge T. Yoshida, Y. Kohsaka, T. Machida, and C. J. Butler for discussion. This work was supported by Grant-in-Aid JSPS KAKENHI Grants No. JP19H01855, No. JP21H04652, No. JP21H05236, No. JP21K18181, No. JP22H04496, and No. JP22H05448.

[1] H. S. Jarrett, W. H. Cloud, R. J. Bouchard, S. R. Butler, C. G. Frederick, and J. L. Gillson, Evidence for itinerant *d*-electron ferromagnetism, Phys. Rev. Lett. **21**, 617 (1968).

[2] T. A. Bither, R. Bouchard, W. Cloud, P. Donohue, and W. Siemons, Transition metal pyrite dichalcogenides. High-pressure synthesis and correlation of properties, Inorg. Chem. **7**, 2208 (1968).

[3] S. Ogawa, Magnetic properties of 3d transition-metal dichalcogenides with the pyrite structure, J. Appl. Phys. **50**, 2308 (1979).

[4] M. Imada, A. Fujimori, and Y. Tokura, Metal-insulator transitions, Rev. Mod. Phys. **70**, 1039 (1998).

[5] X. Yao, J. M. Honig, T. Hogan, C. Kannewurf, and J. Spałek, Electrical properties of $NiS_{2-x}Se_x$ single crystals: From Mott insulator to paramagnetic metal, Phys. Rev. B **54**, 17469 (1996).

[6] S. Miyasaka, H. Takagi, Y. Sekine, H. Takahashi, N. Mri, and R. J. Cava, Metal-insulator transition and itinerant antiferromagnetism in $NiS_{2-x}Se_x$ pyrite, J. Phys. Soc. Jpn. **69**, 3166 (2000).

[7] H. C. Xu, Y. Zhang, M. Xu, R. Peng, X. P. Shen, V. N. Strocov, M. Shi, M. Kobayashi, T. Schmitt, B. P. Xie, and D. L. Feng, Direct observation of the bandwidth control Mott transition in the $NiS_{2-x}Se_x$ multiband system, Phys. Rev. Lett. **112**, 087603 (2014).

[8] G. Han, S. Choi, H. Cho, B. Sohn, J.-G. Park, and C. Kim, Structural investigation of the insulator-metal transition in $NiS_{2-x}Se_x$ compounds, Phys. Rev. B **98**, 125114 (2018).

[9] B. G. Jang, G. Han, I. Park, D. Kim, Y. Y. Koh, Y. Kim, W. Kyung, H.-d. Kim, C.-m. Cheng, K.-d. Tsuei, K. D. Lee,

N. Hur, J. H. Shim, C. Kim, and G. Kotliar, Direct observation of kink evolution due to Hund's coupling on approach to metal-insulator transition in $NiS_{2-x}S_x$, Nat. Commun. **12**, 1208 (2021).

[10] S. Friedemann, H. Chang, M. Gamża, P. Reiss, X. Chen, P. Alireza, W. Coniglio, D. Graf, S. Tozer, and F. Grosche, Large Fermi surface of heavy electrons at the border of Mott insulating state in NiS_2, Sci. Rep. **6**, 25335 (2016).

[11] T. Hussain, M.-j. Oh, M. Nauman, Y. Jo, G. Han, C. Kim, and W. Kang, Pressure-induced metal–insulator transitions in chalcogenide $NiS_{2-x}Se_x$, Phys. B: Condens. Matter **536**, 235 (2018).

[12] K. Momma and F. Izumi, *Vesta 3* for three-dimensional visualization of crystal, volumetric and morphology data, J. Appl. Cryst. **44**, 1272 (2011).

[13] A. Jain, S. P. Ong, G. Hautier, W. Chen, W. D. Richards, S. Dacek, S. Cholia, D. Gunter, D. Skinner, G. Ceder, and K. A. Persson, Commentary: The materials project: A materials genome approach to accelerating materials innovation, APL Mater. **1**, 011002 (2013).

[14] T. Thio and J. W. Bennett, Hall effect and conductivity in pyrite NiS_2, Phys. Rev. B **50**, 10574 (1994).

[15] K. Rao, T. Bhuvana, B. Radha, N. Kurra, N. Vidhyadhiraja, and G. Kulkarni, Metallic conduction in NiS_2 nanocrystalline structures, J. Phys. Chem. C **115**, 10462 (2011).

[16] C. Clark and S. Friedemann, Atomic diffusion in the surface state of Mott insulator NiS_2, J. Magn. Magn. Mater. **400**, 56 (2016).

[17] T. Thio, J. W. Bennett, and T. R. Thurston, Surface and bulk magnetic properties of pyrite NiS_2: Magnetization and neutron-scattering studies, Phys. Rev. B **52**, 3555 (1995).

[18] D. D. Sarma, S. R. Krishnakumar, E. Weschke, C. Schüßler-Langeheine, C. Mazumdar, L. Kilian, G. Kaindl, K. Mamiya, S.-I. Fujimori, A. Fujimori, and T. Miyadai, Metal-insulator crossover behavior at the surface of NiS_2, Phys. Rev. B **67**, 155112 (2003).

[19] S. El-Khatib, B. Voigt, B. Das, A. Stahl, W. Moore, M. Maiti, and C. Leighton, Conduction via surface states in antiferromagnetic Mott-insulating NiS_2 single crystals, Phys. Rev. Mater. **5**, 115003 (2021).

[20] R. Hartmann, M. Hgen, D. Lignon, A. K. Tan, M. Amado, S. El-Khatib, M. Egilmez, B. Das, C. Leighton, M. Atatre, E. Scheer, and A. Di Bernardo, Intrinsic giant magnetoresistance due to exchange-bias-type effects at the surface of single-crystalline NiS_2 nanoflakes, Nanoscale **15**, 10277 (2023).

[21] S. El-Khatib, F. Mustafa, M. Egilmez, B. Das, Y. Tao, M. Maiti, Y. Lee, and C. Leighton, Exotic surface magnetotransport phenomena in the antiferromagnetic Mott insulator NiS_2, Phys. Rev. Mater. **7**, 104401 (2023).

[22] K. Iwaya, Y. Kohsaka, S. Satow, T. Hanaguri, S. Miyasaka, and H. Takagi, Evolution of local electronic states from a metal to a correlated insulator in a $NiS_{2-x}Se_x$ solid solution, Phys. Rev. B **70**, 161103(R) (2004).

[23] P. Kwizera, M. S. Dresselhaus, and D. Adler, Electrical properties of $NiS_{2-x}Se_x$, Phys. Rev. B **21**, 2328 (1980).

[24] R. L. Kautz, M. S. Dresselhaus, D. Adler, and A. Linz, Electrical and optical properties of NiS_2, Phys. Rev. B **6**, 2078 (1972).

[25] A. Y. Matsuura, H. Watanabe, C. Kim, S. Doniach, Z.-X. Shen, T. Thio, and J. W. Bennett, Metal-insulator transition in $NiS_{2-x}Se_x$ and the local impurity self-consistent approximation model, Phys. Rev. B **58**, 3690 (1998).

[26] G. Lantz, M. Hajlaoui, E. Papalazarou, V. L. R. Jacques, A. Mazzotti, M. Marsi, S. Lupi, M. Amati, L. Gregoratti, L. Si, Z. Zhong, and K. Held, Surface effects on the Mott-Hubbard transition in archetypal V_2O_3, Phys. Rev. Lett. **115**, 236802 (2015).

[27] S. Tang, C. Zhang, D. Wong, Z. Pedramrazi, H.-Z. Tsai, C. Jia, B. Moritz, M. Claassen, H. Ryu, S. Kahn, J. Jiang, H. Yan, M. Hashimoto, D. Lu, R. G. Moore, C.-C. Hwang, C. Hwang, Z. Hussain, Y. Chen, M. M. Ugeda *et al.*, Quantum spin Hall state in monolayer 1T'-WTe_2, Nat. Phys. **13**, 683 (2017).

[28] F. Schindler, Z. Wang, M. G. Vergniory, A. M. Cook, A. Murani, S. Sengupta, A. Y. Kasumov, R. Deblock, S. Jeon, I. Drozdov, H. Bouchiat, S. Guron, A. Yazdani, B. A. Bernevig, and T. Neupert, Higher-order topology in bismuth, Nat. Phys. **14**, 918 (2018).

[29] Y. Xu, L. Elcoro, Z.-D. Song, B. J. Wieder, M. G. Vergniory, N. Regnault, Y. Chen, C. Felser, and B. A. Bernevig, High-throughput calculations of magnetic topological materials, Nature (London) **586**, 702 (2020).

[30] N. Shumiya, M. S. Hossain, J. X. Yin, Z. Wang, M. Litskevich, C. Yoon, Y. Li, Y. Yang, Y. X. Jiang, G. Cheng, Y. C. Lin, Q. Zhang, Z. J. Cheng, T. A. Cochran, D. Multer, X. P. Yang, B. Casas, T. R. Chang, T. Neupert, Z. Yuan *et al.*, Evidence of a room-temperature quantum spin Hall edge state in a higher-order topological insulator, Nat. Mater. **21**, 1111 (2022).

[31] J.-X. Yin, Y.-X. Jiang, X. Teng, M. S. Hossain, S. Mardanya, T.-R. Chang, Z. Ye, G. Xu, M. M. Denner, T. Neupert, B. Lienhard, H.-B. Deng, C. Setty, Q. Si, G. Chang, Z. Guguchia, B. Gao, N. Shumiya, Q. Zhang, T. A. Cochran *et al.*, Discovery of charge order and corresponding edge state in kagome magnet FeGe, Phys. Rev. Lett. **129**, 166401 (2022).

[32] M. Bronold, Y. Tomm, and W. Jaegermann, Surface states on cubic d-band semiconductor pyrite (FeS_2), Surf. Sci. **314**, L931 (1994).

[33] F. W. Herbert, A. Krishnamoorthy, K. J. Van Vliet, and B. Yildiz, Quantification of electronic band gap and surface states on FeS_2(100), Surf. Sci. **618**, 53 (2013).

[34] M. Limpinsel, N. Farhi, N. Berry, J. Lindemuth, C. L. Perkins, Q. Lin, and M. Law, An inversion layer at the surface of n-type iron pyrite, Energy Environ. Sci. **7**, 1974 (2014).

[35] J. Walter, X. Zhang, B. Voigt, R. Hool, M. Manno, F. Mork, E. S. Aydil, and C. Leighton, Surface conduction in *n*-type pyrite FeS_2 single crystals, Phys. Rev. Mater. **1**, 065403 (2017).

[36] J. Walter, B. Voigt, E. Day-Roberts, K. Heltemes, R. M. Fernandes, T. Birol, and C. Leighton, Voltage-induced ferromagnetism in a diamagnet, Sci. Adv. **6**, eabb7721 (2020).

[37] N. Wu, R. F. Sabirianov, W.-N. Mei, Y. B. Losovyj, N. Lozova, M. Manno, C. Leighton, and P. A. Dowben, The minority spin surface bands of CoS_2(001), J. Phys.: Condens. Matter **21**, 295501 (2009).

[38] N. B. M. Schroter, I. Robredo, S. Klemenz, R. J. Kirby, J. A. Krieger, D. Pei, T. Yu, S. Stolz, T. Schmitt, P. Dudin, T. K. Kim, C. Cacho, A. Schnyder, A. Bergara, V. N. Strocov, F. de Juan, M. G. Vergniory, and L. M. Schoop, Weyl fermions, Fermi arcs, and minority-spin carriers in ferromagnetic CoS_2, Sci. Adv. **6**, eabd5000 (2020).